Research on the Operation Plan of Urban Rail Transit and Suburban Railway Connection

Shuoyue Gao, Changfeng Zhu, Yunqi Fu, Jie Wang, Linna Cheng, and Rongjie Kuang

Abstract—**To improve through operation (TO) plans between urban rail transit (URT) and suburban railway (SR) systems, this study overcomes the limitations of traditional transfer modes in handling peak-hour cross-line (CL) passenger demand. We develop a passenger choice behavior model integrating cumulative prospect theory (CPT) and quantum decision theory (QDT). This model quantifies passenger decision-making under multi-attribute trade-offs (time, cost, comfort). A TO optimization model is established with dual objectives: minimizing passenger travel time and reducing operator costs. We propose a chaos-enhanced non-dominated sorting genetic algorithm (CNSGA) with opposition-based learning for solution derivation. Case study results show that TO schemes reduce total passenger travel time by 60.7% and operational costs by 30.1% compared to transfer-based connections. Sensitivity analysis reveals two key findings: (1) Passengers with higher time-value sensitivity prefer TO trains more strongly; (2) A higher proportion of such passengers improves the time-saving benefits of TO optimization. Although skip-stop strategies improve travel time for TO flows, they may negatively impact other passenger groups. This study provides a theoretical foundation for coordinated planning in hierarchical rail networks.**

Index Terms—**Urban Rail Transit, Suburban Railway, Operation Plan, Cumulative Prospect Theory, Quantum Decision Theory**

I. INTRODUCTION

WITH accelerating global urbanization, suburban areas of metropolitan regions are becoming strategic hinterlands for population decentralization and industrial relocation [1], [2]. This trend creates substantial commuter demand between urban cores and suburbs, placing significant pressure on transportation systems. Tokyo Metropolitan Area data show daily cross-regional commuter volumes reach 2.86 million person-trips [3]. Conventional solutions involve building high-density urban rail transit (URT) networks in city centers and suburban railway (SR) systems in peripheral regions. Transfer hubs connect these systems.

However, this line-separation mode has significant limitations. As metropolitan regions expand and commuting distances increase, traditional transfer systems struggle to meet peak-hour CL passenger flow demands. Consequently, scholars proposed the TO mode. TO achieves functional complementarity and resource sharing across multi-level rail transit systems. It transcends traditional boundaries, enabling seamless cross-system train operations via URT-SR line interconnections. Existing research addresses three main aspects:

Firstly, in the aspect of TO feasibility analysis, early studies focused mainly on optimizing single-level rail transit operations, often neglecting network coordination. With urban agglomeration and longer commutes, scholars proposed multi-level integrated operation modes emphasizing functional synergy. Examples include: Vigrass et al. [4] investigating power supply for URT-SR interoperability; Drechsler [5] analyzing shared-track operations in Karlsruhe; Sato [6] examining Tokyo's TO impact on Paris RER; and Novales et al. [7] identifying technical challenges for trams on conventional railways.

Secondly, in terms of TO train plan optimization, Tang et al. [8], [9] developed mixed-integer linear programming models for express-local train scheduling under different capacity conditions. Paebo et al. [10] proposed a bi-level model for optimal skip-stop patterns considering passenger behavior. Altazin et al. [11] used skip-stop to minimize service recovery time. Shang et al. [12], [13] investigated passenger equity in oversaturated networks. Later studies advanced nonlinear programming for coordinated optimization: Yang et al. [14], [15] used MINLP to quantify express train benefits; Tang et al. [16] optimized scheduling via station classification and flow allocation; Li et al. [17] developed MINLP for stop patterns and dwell times; Chen et al. [18] proposed nonlinear models minimizing deviations under dynamic flows; Shao et al. [19] integrated timetabling and stop planning with equity.

Regarding algorithmic approaches, traditional methods like GA, SA, and PSO have limitations: slow convergence and susceptibility to local optima. Recent advances incorporated chaotic and quantum mechanisms. Zhu et al. [20], [21] developed a chaos-based non-dominated sorting GA (CNSGA). Jiao et al. [22], [23], [24] created adaptive chaotic PSO with opposition-based learning.

Manuscript received April 25, 2025; revised July 11, 2025.

This work was supported in part by the National Natural Science Foundation of China (No.72161024) and "Double-First Class" Major Research Programs, Educational Department of Gansu Province (No.GSSYLXM-04).

Shuoyue Gao is a postgraduate student at School of Traffic and Transportation, Lanzhou Jiaotong University, Lanzhou 730070, China (e-mail: 18049395600@163.com).

Changfeng Zhu is a professor at School of Traffic and Transportation, Lanzhou Jiaotong University, Lanzhou 730070, China (Corresponding author, phone: +86 189 1989 1566, e-mail: cfzhu003@163.com).

Yunqi Fu is a doctoral candidate at School of Traffic and Transportation, Lanzhou Jiaotong University, Lanzhou 730070, China (e-mail: 13240002@stu.lzjtu.edu.cn).

Jie Wang is a doctoral candidate at School of Traffic and Transportation, Lanzhou Jiaotong University, Lanzhou 730070, China (e-mail: 1009696615@qq.com).

Linna Cheng is a doctoral candidate at School of Traffic and Transportation, Lanzhou Jiaotong University, Lanzhou 730070, China (e-mail: chengjj @163.com).

Rongjie Kuang is a doctoral candidate at School of Traffic and Transportation, Lanzhou Jiaotong University, Lanzhou 730070, China (e-mail: kuangrj@126.com).

Thirdly, analysis of passenger travel behavior. Discrete choice models (e.g., MNL) and expected utility theory dominate research. However, their assumption of complete rationality contradicts actual passenger decision-making influenced by socioeconomic factors and bounded rationality. Cumulative prospect theory (CPT) addresses this limitation [25], [26], applied in route choice [27], [28], [29], travel time uncertainty [30], [31], and multi-attribute tradeoffs [32]. To handle multi-attribute decisions (time, cost, comfort), quantum decision theory (QDT) complements CPT. QDT conceptualizes decisions as probabilistic belief states, shown by Martínez-Martínez [33] (Hamiltonian interactions), Yukalov and Sornette [34] (quantum frameworks), and Pothos and Busemeyer [35] (quantum cognition).

Despite progress, current research on multi-level rail networks mainly focuses on transfer-based systems, with limited TO exploration. Existing TO studies often oversimplify passenger rationality and neglect multi-attribute behavior. This study addresses these gaps with three key contributions:

(i) We develop a CPT-QDT integrated passenger travel choice model. CPT captures train selection under bounded rationality, while QDT quantifies travel mode choice probabilities.

(ii) We establish a multi-objective TO train operation model considering passenger time value. It minimizes travel and operating costs under constraints (passenger flow, occupancy, frequency, station capacity).

(iii) We design a CNSGA incorporating opposition-based learning. Logistic chaotic mapping improves traditional algorithms to find optimal strategy sets.

The paper is organized as follows: Section II analyzes passenger travel choice under bounded rationality; Section III develops the TO operation model; Section IV details the CNSGA; Section V presents case studies; Section VI conducts sensitivity analysis; Section VII concludes.

II. Passenger Travel Choice Model Based on CPT-QDT

Assume the travel mode set $H=\{h|g,b\}$, where g and b represent passengers choosing through trains and local trains, respectively. Considering passengers' travel choices are influenced by factors such as time and cost, the value of time $vot(h)$ is introduced to convert time into monetary cost. The generalized travel time cost u_{ij}^{h} for choosing travel mode h from station i to station j is

$$u_{ij}^{h}=(T_{ij,\mathrm{w}}^{h}+T_{\mathrm{z}})\cdot vot(h)+z_{ij}^{h} \tag{1}$$

Where, $T_{ij,\mathrm{w}}^{h}$ denotes the waiting time for travel mode h between stations i and j; T_{z} denotes the transfer time; Z_{ij}^{h} indicates the cost (yuan) of travel mode h from station i to j; $vot(h)$ denotes the value of time coefficient (yuan/min) for mode h.

Considering passengers' travel decisions are influenced by factors such as time and comfort level, value functions for time and crowding degree are constructed, denoted as $v(u_{ij}^{h})$ and $v(c_{ij}^{h})$, respectively.

$$v(u_{ij}^{h},u_{ij}^{0})=\begin{cases}(\Delta u_{ij})^{\alpha} & ,\Delta u_{ij}\geq 0\\ -\chi(-\Delta u_{ij})^{\beta} & ,\Delta u_{ij}<0\end{cases} \tag{2}$$

$$v(c_{ij}^{h},c_{ij}^{0})=\begin{cases}(c_{ij}^{0}-c_{ij}^{h})^{\alpha}, & c_{ij}^{h}\leq c_{ij}^{0}\\ -\chi(c_{ij}^{h}-c_{ij}^{0})^{\beta}, & c_{ij}^{h}>c_{ij}^{0}\end{cases} \tag{3}$$

Where, α denotes the gain sensitivity coefficient, $0\leq\alpha\leq 1$; β denotes the loss sensitivity coefficient, $0\leq\beta\leq 1$; χ denotes the loss aversion coefficient; u_{ij}^{0} and c_{ij}^{0} denote the reference points for travel time and crowding degree, with values corresponding to the generalized travel time cost before the implementation of through trains and the average crowding level across travel modes, respectively; c_{ij}^{h} denotes the crowding degree of travel mode h from station i to j station.

The decision function $\omega(l_{ij}^{h})$ is expressed as

$$\omega(l_{ij}^{h})=\frac{\sigma(l_{ij}^{h})^{\rho}}{(1-l_{ij}^{h})^{\rho}+\sigma(l_{ij}^{h})^{\rho}},\rho>1 \tag{4}$$

Where, σ denotes the discriminability parameter; ρ denotes the attractiveness parameters.

Assuming passenger travel decisions primarily depend on two factors—travel time T and comfort level Y, the cumulative prospect value U_{od}^{Th} for travel time and the cumulative prospect value U_{ij}^{Yh} for crowding intensity under travel mode h are calculated as

$$U_{ij}^{Th}=v(u_{ij}^{h})\cdot\omega(l_{ij}^{h}) \tag{5}$$

$$U_{ij}^{Yh}=\omega(l_{ij}^{h})\cdot v(c_{ij}^{h}) \tag{6}$$

Each subspace in Hilbert space is represented by a set of measurement events $|Z\rangle$, and the $|Z\rangle$ projection on the coordinate axis ψ_h represents the potential motivation $|\psi_h|$ of each option. The square of its length is the probability value corresponding to that option. The schematic diagram of Hilbert two-dimensional space is shown in Fig. 1.

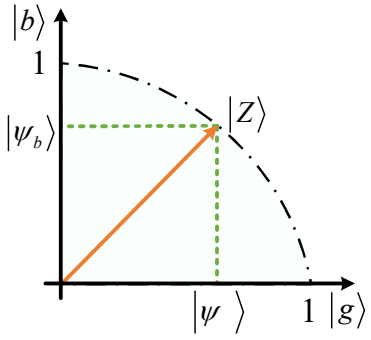

Fig.1. Schematic diagram in Hilbert two-dimensional space.

According to Fig. 1, in the initial state, the decision-maker may choose either the through train g or the local train b; these two options are represented by vectors $|g\rangle$ and $|b\rangle$, respectively. ψ_g and ψ_b denote the projections of $|Z\rangle$ on the $|g\rangle$ and $|b\rangle$ coordinate axes. The longer the projections $|\psi_g|$ and $|\psi_b|$, the higher the probability of the option being

selected. However, when multiple attributes (time T, comfort Y) jointly act on $|Z\rangle$, the state of $|Z\rangle$ will change. A schematic diagram of belief state variation is illustrated in Fig. 2.

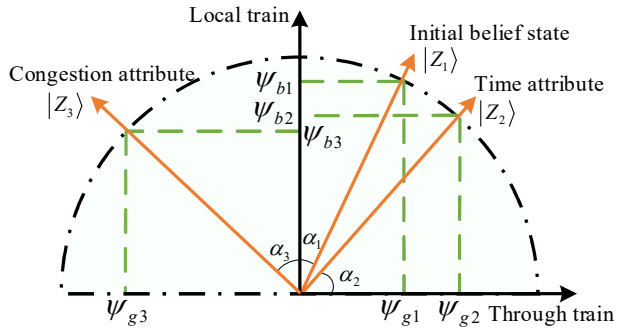

Fig.2. Schematic diagram of changes in belief state.

According to Fig. 2, the initial belief state $|Z_1\rangle$ evolves under the influence of T and Y. This evolution is quantified by the vector angle α, resulting in a superposition of states $|Z_2\rangle$ and $|Z_3\rangle$. For the choice alternatives $Alt_h = \{|g\rangle, |b\rangle\}$ under travel option h, the selection probability P_{ij}^h is given by the squared modulus of the alternative across decision attributes. Specifically:

$$P_{ij}^h = |P_{x_h}|Z\rangle|^2 = |\langle Z|x_h\rangle|^2 = |\psi_{ij}^h|^2 \quad (7)$$

Where, $P_{x_h}|Z\rangle$ denotes the probability of selecting travel mode h under belief state $|Z\rangle$; ψ_{ij}^h denotes the amplitude of passengers traveling from station i to j choosing mode h; x_h denotes the vector state of travel mode h; $P_{x_h}|Z\rangle$ denotes the passenger's choice belief state.

For each passenger, among the given choice attributes, the projection ψ_{ij}^h of option h is estimated as the cumulative sum of subjective differences relative to other options. That is

$$\psi_{ij}^g = (\delta_g + \sum_{i\neq j} \Delta_{ij}^{bg}) / \sqrt{N} \quad (8)$$

Where, Δ_{od}^{bg} denotes the subjective difference between option g and option b for passengers traveling from i to j; δ_g denotes the error term of option g; $\sqrt{N}$ denotes the normalization factor, calculated as the sum of squared moduli.

Assuming the attribute set $C = \{c|T, Y\}$ influencing choice behavior, the subjective difference Δ_{ij}^{gb} between different options is computed using a linear difference function

$$\Delta_{ij}^{gb} = \sum_{c=1}^{C} \beta_c \cdot (U_{ij}^{cg} - U_{ij}^{cb}) \quad (9)$$

Where, β_c denotes the relative importance coefficient of attribute c; U_{od}^{ck} denotes the prospect value of attribute c for through-train passengers; U_{od}^{cb} denotes the prospect value of attribute c for local-train passengers.

The probability P_{ij}^h of choosing different modes of transportation h is

$$P_{ij}^h = |\psi_{ij}^h|^2 = \left| \frac{(\delta_h + \sum_{b\neq g} \Delta_{bg})}{\sqrt{\sum_{h=g}^{b} |\delta_h + \sum_{g\neq b}^{b} \Delta_{bg}|^2}} \right|^2 \quad (10)$$

III. Mathematical Model

A. Problem Assumptions

The following assumptions are made:

(1) All passengers arrive approximately in a random Poisson distribution per unit time, and passengers transfer at most once, without considering passenger congestion.

(2) Passenger travel directions, origin-destination characteristics, and OD passenger flows between stations remain constant within the study scope.

(3) All trains operate with all-stop patterns, single routing configurations, fixed formation sizes, and identical turn-back times.

B. Problem Description

Let URT line L_S have station set $s = \{1, 2, ..., a, ..., m\}$, and SR line L_R' station set $r = \{m+1, m+2, ..., b, ..., n\}$. The two rail lines connect at station m. Local trains of types S and R operate on lines L_S and L_R respectively. During peak hours, a large number of CL passenger flows from line L_S to line L_R require transfers at connecting station m. To mitigate transfer inconveniences for passengers and operators, through trains operate between station a and station b. All three train types maintain all-stop patterns, with the analysis period set as one peak hour. URT and SR train operation under the TO mode is shown in Fig. 3.

Based on the operation routes of three types of trains, lines L_S and L_R are divided into four sections: $D_1 = [1, a)$, $D_2 = [a, m)$, $D_3 = [m, b)$, and $D_4 = [b, n]$. Specifically, sections D_1 and D_4 are exclusively operated by local trains, while sections D_2 and D_3 accommodate both local trains and TO trains.

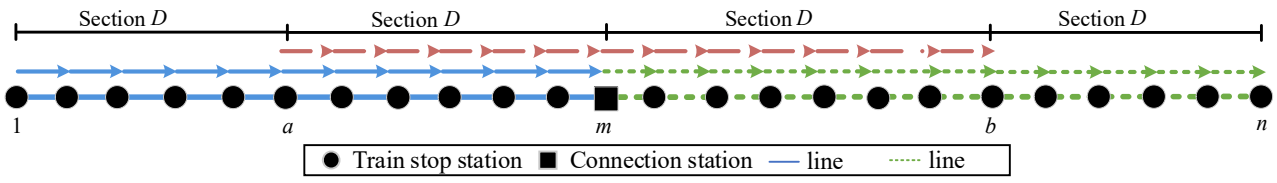

Fig.3. URT and SR train operation under the TO mode.

C. Objective Function Analysis

(1) Passenger travel time function

The total passenger travel time T comprises waiting time, transfer time, and in-vehicle time. The waiting time can be approximated as half of the departure interval, and the waiting time T_{ij}^{w} for passengers traveling from station i to j is given by

$$T_{ij}^{\mathrm{w}} = 30/f_k, k = 1,2,3 \tag{11}$$

Where, f_1、f_2、f_3 denote the departure frequencies (/hour) of train S, through-operation trains, and train R, respectively.

A transfer penalty coefficient τ is introduced to quantify the time and physical effort associated with transfers. The transfer time T_q^{h} at transfer station q can be expressed as

$$T_q^{\mathrm{h}} = \tau \cdot ((D_q / V_q) + w_q), \forall q \in (s \cup r) \tag{12}$$

Where, D_q, w_q, V_q respectively denote the waiting time, average walking distance, and average walking speed of passengers at transfer station q.

The in-vehicle time includes both train running time and dwell time. The in-vehicle time T_{ij}^{z} for passengers traveling from station i to j is given by

$$T_{ij}^{z} = \sum_{i=1}^{j-1} t_i^{\mathrm{run}} + \sum_{i=2}^{j} x_i \cdot t_i^{\mathrm{stop}} \tag{13}$$

Where, t_i^{run} denotes the pure running time in section $[i, i+1]$; x_i denotes whether through-operation trains stop at station i (1 for stopping, 0 otherwise); t_i^{stop} denotes the train dwelling time at station i.

The overall travel time cost T for passengers is

$$\begin{aligned} T = &\sum_{i=1}^{n-1} \sum_{j=i+1}^{n} (T_{ij}^{\mathrm{w,H}} + T_{ij}^{\mathrm{h,H}} + T_{ij}^{\mathrm{z,H}}) + (T_{ij}^{\mathrm{w,C}} \\ &+ T_{ij}^{\mathrm{h,C}} + T_{ij}^{\mathrm{z,C}}) + \xi \cdot (\psi \cdot \mu \cdot z_{ij} / \Omega) \end{aligned} \tag{14}$$

Where, $T_{ij}^{\mathrm{w,H}}$, $T_{ij}^{\mathrm{w,C}}$ denote the waiting times for passengers traveling from station i to j via local route H and C respectively; $T_{ij}^{\mathrm{h,H}}$, $T_{ij}^{\mathrm{h,C}}$ denote the transfer times for H-route and C-route passengers; $T_{ij}^{\mathrm{z,H}}$, $T_{ij}^{\mathrm{z,C}}$ denote the in-vehicle times for H-route and C-route passengers; ξ denotes the cost conversion weight reflecting passengers' sensitivity differences between travel time and fare, set based on income and trip purpose; ψ denotes the daily working hours; μ denotes the statutory working days; z_{ij} denotes the ticket fare for passengers traveling from station i to j; Ω denotes the annual per capita income.

The passenger flow types on lines $\mathrm{L_S}$ and $\mathrm{L_R}$ include passengers traveling only on the local line (denoted as H) and CL passengers (denoted as C). The local line passenger flow is further divided into four categories: HMM, HMK, HKM, HKK; the CL passenger flow is also divided into four categories: CMM, CMK, CKM, CKK. The classification of passenger flow types is shown in Fig. 4.

Among them, the local line passenger flow (H) is divided into the following two cases: case1a and case1b, while the CL passenger flow (C) includes: case2a and case2b, specifically:

Case 1a: HMM and HKK represent passenger flows within the local line section with origin-destination stations both being M or K, choosing only local trains or through-operation trains. The travel times T_{ij}^{HMM}, T_{ij}^{HKK} for HMM and HKK are

$$\begin{cases} T_{ij}^{\mathrm{HMM}} = x_i \cdot x_j \cdot q_{ij} \cdot T_{ij,\mathrm{w}}^{\mathrm{HMM}} + T_{ij,\mathrm{z}}^{\mathrm{HMM}} \\ \quad + \xi \cdot (a \cdot q \cdot z_{ij} / x) \\ T_{ij}^{\mathrm{HKK}} = (1 - x_i \cdot x_j) \cdot q_{ij} \cdot (p_{ij}^{b} \cdot T_{ij,\mathrm{w}}^{\mathrm{HKK},b} \\ \quad + p_{ij}^{g} \cdot T_{ij,\mathrm{w}}^{\mathrm{HKK},g}) + T_{ij,\mathrm{z}}^{\mathrm{HKK}} + \xi \cdot (a \cdot q \cdot z_{ij} / x) \\ T_{ij,\mathrm{w}}^{\mathrm{HKK},b} = 30/f_k, \quad k=\{1,3\} \\ T_{ij,\mathrm{w}}^{\mathrm{HKK},g} = 30/f_2 \end{cases} \tag{15}$$

Case 1b: HMK and HKM represent passenger flows within the local line section with origin/destination stations being M or K. The travel times T_{ij}^{HMK}, T_{ij}^{HKM} for HMK and HKM are

$$\begin{cases} T_{ij}^{\mathrm{HMK}} = x_i \cdot (1 - x_j) \cdot q_{ij} \cdot (p_{ij}^{b} \cdot T_{ij,\mathrm{w}}^{\mathrm{HMK},b} \\ \quad + p_{ij}^{g} \cdot T_{ij,\mathrm{w}}^{\mathrm{HMK},g}) + T_{ij,\mathrm{z}}^{\mathrm{HMK}} + \xi \cdot (a \cdot q \cdot z_{ij} / x) \\ T_{ij}^{\mathrm{HKM}} = (1 - x_i) \cdot x_j \cdot q_{ij} \cdot (p_{ij}^{b} \cdot T_{ij,\mathrm{w}}^{\mathrm{HKM},b} \\ \quad + p_{ij}^{g} \cdot T_{ij,\mathrm{w}}^{\mathrm{HKM},g}) + T_{ij,\mathrm{z}}^{\mathrm{HKM}} + \xi \cdot (a \cdot q \cdot z_{ij} / x) \\ T_{ij,\mathrm{w}}^{\mathrm{HMK},b} = 30/f_k, \quad k=\{1,3\} \\ T_{ij,\mathrm{w}}^{\mathrm{HMK},g} = (30/f_k) + (30/f_2), \quad k=\{1,3\} \end{cases} \tag{16}$$

Case 2a: CMM and CKK represent CL passenger flows with origin-destination stations both being M or K. These passengers only take local trains or TO trains with one transfer. The travel times T_{ij}^{CMM}, T_{ij}^{CKK} for CMM and CKK are

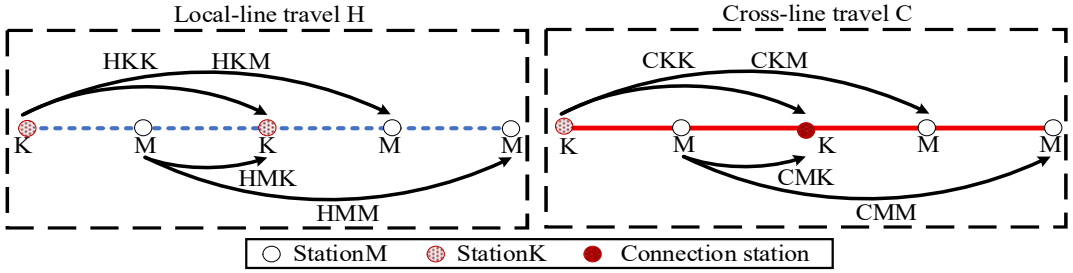

Fig.4. Passenger travel type classification.

$$\begin{cases} T_{ij}^{\mathrm{CMM}} = x_i \cdot x_j \cdot q_{ij} \cdot (T_{ij,\mathrm{w}}^{\mathrm{CMM}} + T_{ij,\mathrm{h}}^{\mathrm{CMM}}) + T_{ij,\mathrm{z}}^{\mathrm{CMM}} \\ +\xi \cdot (a \cdot q \cdot z_{ij} / x) \\ T_{ij}^{\mathrm{CKK}} = (1 - x_i \cdot x_j) q_{ij} \cdot (T_{ij,\mathrm{w}}^{\mathrm{CKK}} + T_{ij,\mathrm{h}}^{\mathrm{CKK}} + T_{ij,\mathrm{z}}^{\mathrm{CKK}}) \\ +\xi \cdot (a \cdot q \cdot z_{ij} / x) \\ T_{ij,w}^{\mathrm{CMM}} = (30/f_1) + (30/f_3) \\ T_{ij,\mathrm{w}}^{\mathrm{CKK}} = 30/f_2 \end{cases} \tag{17}$$

Case 2b: CMK and CKM represent CL passenger flows with origin/destination stations being M or K. The travel times T_{ij}^{CMK}, T_{ij}^{CKM} for CMK and CKM are

$$\begin{cases} T_{ij}^{\mathrm{CMK}} = x_i \cdot (1 - x_j) \cdot q_{ij} \cdot (p_{ij}^{b} \cdot T_{ij,\mathrm{w}}^{\mathrm{CMK},b} \\ + p_{ij}^{g} \cdot T_{ij,\mathrm{w}}^{\mathrm{CMK},g} + T_{ij,\mathrm{z}}^{\mathrm{CMK}}) + \xi \cdot (a \cdot q \cdot z_{ij} / x) \\ T_{ij}^{\mathrm{CKM}} = (1 - x_i) \cdot x_j \cdot q_{ij} \cdot (p_{ij}^{b} \cdot T_{ij,\mathrm{w}}^{\mathrm{CKM},b} \\ + p_{ij}^{g} \cdot T_{ij,\mathrm{w}}^{\mathrm{CKM},g} + T_{ij,\mathrm{z}}^{\mathrm{CKM}}) + \xi \cdot (a \cdot q \cdot z_{ij} / x) \\ T_{ij,\mathrm{w}}^{\mathrm{CMK},b} = 30/f_k, \qquad k=\{1,3\} \\ T_{ij,\mathrm{w}}^{\mathrm{CMK},g} = (30/f_k) + (30/f_2), \qquad k=\{1,3\} \end{cases} \tag{18}$$

Therefore, the travel times T_{ij}^{H}, T_{ij}^{C} for local line passenger flow (H) and CL passenger flow (C) are respectively

$$T_{ij}^{\mathrm{H}} = T_{ij}^{\mathrm{HMM}} + T_{ij}^{\mathrm{HMK}} + T_{ij}^{\mathrm{HKM}} + T_{ij}^{\mathrm{HKK}} \tag{19}$$

$$T_{ij}^{\mathrm{C}} = T_{ij}^{\mathrm{CMM}} + T_{ij}^{\mathrm{CMK}} + T_{ij}^{\mathrm{CKM}} + T_{ij}^{\mathrm{CKK}} \tag{20}$$

Through comprehensive analysis, the objective function Z2 aims at minimizing passengers' total travel time T.

$$Z2 = \min \sum_{i=1}^{n-1} \sum_{j=i+1}^{n} T_{ij}^{\mathrm{H}} + T_{ij}^{\mathrm{C}} + \xi \cdot (a \cdot q \cdot z_{ij} / x) \tag{21}$$

(2) Enterprise operating cost function

Transport operator costs include fixed costs and variable costs. Fixed costs only consider vehicle procurement and depreciation costs, while variable costs include operation costs related to train frequency. The fixed costs Z_{sc}, Z_{rc} for lines $\mathrm{L_S}$, $\mathrm{L_R}$ are respectively

$$Z_{\mathrm{sc}} = (f_1 B_1 T_1 + f_2 B_2 T_2) C_s \tag{22}$$

$$Z_{\mathrm{rc}} = f_3 B_3 T_3 C_r \tag{23}$$

Where, B_1, B_2, B_3 denote the fixed formation numbers of three types of trains (/unit) respectively; T_1, T_2, T_3 denote the turnaround times of three types of trains respectively; C_s, C_r denote the fixed vehicle costs per unit time (/yuan) on lines $\mathrm{L_S}$, $\mathrm{L_R}$ respectively.

Among them, train turnaround time includes running time between sections, dwell time at stations, and turn-back time. The turnaround times T_1, T_2, T_3 for the three types of trains are respectively

$$T_1 = \frac{(\sum_{i=1}^{m-1} t_{irun} + \sum_{i=2}^{m-1} t_{istop})}{3600} + \frac{t_{turn}}{60} \tag{24}$$

$$T_2 = \frac{(\sum_{i=a}^{b-1} t_{irun} + \sum_{i=a+1}^{b-1} t_{istop})}{3600} + \frac{t_{turn}}{60} \tag{25}$$

$$T_3 = \frac{(\sum_{i=m}^{n-1} t_{irun} + \sum_{i=m+1}^{n-1} t_{istop})}{3600} + \frac{t_{turn}}{60} \tag{26}$$

Where, t_{irun} denotes running time in section [i, i+1] (s); t_{istop} indicates dwell time at station i (s); t_{turn} denotes turn-back time at terminal stations (min).

Variable costs relate to train-kilometer operation and service frequency. The unit vehicle-kilometer operating cost for local trains follows local line standards, through-operation trains follow local standards within the local line section and CL standards beyond, thus the variable costs Z_{se}, Z_{re} for lines $\mathrm{L_S}$, $\mathrm{L_R}$ are respectively

$$Z_{\mathrm{se}} = f_1 B_1 e_s \sum_{i=1}^{m-1} L_i + f_2 B_2 e_s \sum_{i=a}^{m-1} L_i + f_2 B_2 e_r \sum_{i=m}^{b-1} L_i \tag{27}$$

$$Z_{\mathrm{re}} = f_3 B_3 e_r \sum_{i=m}^{n-1} L_i \tag{28}$$

Where, e_s, e_r denote system operating costs per vehicle-kilometer (yuan/vehicle-kilometer) on lines $\mathrm{L_S}$, $\mathrm{L_R}$ respectively; L_i denotes station spacing in section [i, i+1] (km).

The total transport enterprise cost Z is expressed as

$$Z = Z_{\mathrm{se}} + Z_{\mathrm{re}} + Z_{\mathrm{sc}} + Z_{\mathrm{rc}} \tag{29}$$

Through comprehensive analysis, the objective functions are set as minimizing enterprise total operating cost Z1 and passenger travel time Z2. That is

$$Z1 = \min Z = (Z_{\mathrm{re}} + Z_{\mathrm{rc}} + Z_{\mathrm{se}} + Z_{\mathrm{sc}}) \tag{30}$$

$$Z2 = \min \sum_{i=1}^{n-1} \sum_{j=i+1}^{n} T_{ij}^{\mathrm{H}} + T_{ij}^{\mathrm{C}} + \xi \cdot (a \cdot q \cdot z_{ij} / x) \tag{31}$$

D. Constraints

(1) Passenger demand constraints. The transportation capacity provided by trains operating in any section must meet all passenger flow demands in that section.

$$\sum_{\substack{i=1 \\ 1 \le k \le a}}^{k} \sum_{j=k+1}^{n} q_{ij} \le \beta_s E_{s1} f_1 \tag{32}$$

$$\sum_{\substack{i=1 \\ a \le k < m}}^{k} \sum_{j=k+1}^{n} q_{ij} \le \beta_s (E_{s1} f_1 + E_{s2} f_2) \tag{33}$$

$$\sum_{\substack{i=1 \\ m \le k < b}}^{k} \sum_{j=k+1}^{n} q_{ij} \le \beta_s (E_{s1} f_1 + E_{s2} f_2) + \beta_r E_{r3} f_3 \tag{34}$$

$$\sum_{\substack{i=1 \\ b \le k \le n}}^{k} \sum_{j=k+1}^{n} q_{ij} \le \beta_s (E_{s1} f_1 + E_{s2} f_2) + \beta_r E_{r3} f_3 \tag{35}$$

Where, β_s, β_r respectively denote the full load rates of S trains and R trains; E_{si} (i=1,2) denote the passenger capacities of S trains and through-operation trains respectively; E_{r3} denotes the passenger capacity of R trains (persons).

(2) Departure frequency constraints. To ensure operational service levels, train frequencies on lines must meet specific requirements. For lines $\mathrm{L_S}$, $\mathrm{L_S}$, the combination of train frequencies must satisfy minimum tracking interval constraints while considering passengers' waiting time should not be excessively long, thus the sum of frequencies for both train types cannot be lower than the line's minimum departure frequency. That is

$$f_{\text{Smin}} \le f_1 + f_2 \le N_{\text{S}}^{\text{cap}} \quad (36)$$

$$f_{\text{Rmin}} \le f_2 + f_3 \le N_{\text{R}}^{\text{Cap}} \quad (37)$$

Where, $N_{\text{S}}^{\text{cap}}$, $N_{\text{R}}^{\text{cap}}$ denote the carrying capacities of lines L_{S}, L_{R} respectively; f_{Smin}, f_{Rmin} denote the minimum departure frequencies for lines L_{S}, L_{R} respectively.

(3) Vehicle utilization constraints. To prevent excessive operational costs, the number of deployed vehicles must meet specific conditions. That is

$$\max\left\{\left\lceil\frac{L_1+t_{zh}V_e}{60V_e}\right\rceil f_1B_1, \left\lceil\frac{L_{21}}{60V_e}\right\rceil f_2B_2\right\} \le B_{\max}. \quad (38)$$

$$\max\left\{\left\lceil\frac{L_3+t_{zh}V_e}{60V_e}\right\rceil f_3B_3, \left\lceil\frac{L_{22}+t_{zh}V_e}{60V_e}\right\rceil f_2B_2\right\} \le B_{\max} \quad (39)$$

Where, L_1, L_2, L_3 denote the routing range lengths (/km) of local train S, through-operation train, and local train R respectively; L_{21}, L_{22} denote the routing range lengths (/km) of $[a,m]$ and $[m,b]$ respectively; $B_{\max}$ denotes the maximum vehicle deployment number (units); V_e denotes train operating speed (km/h); $\lceil\cdot\rceil$ denotes the ceiling function.

(4) Turn-back station capacity constraints. To avoid frequent turn-back operations of through-operation trains at terminals, their departure frequencies must be limited. That is

$$f_2 \le \left\lceil\frac{60}{t_{zh}}\right\rceil, f_2 \in Z^+, \forall f_i \in [f_{\min}, f_{\max}] \quad (40)$$

Where, t_{zh} denotes train turn-back time.

(5) Through-routing range constraints. To ensure through-operation trains turn back at appropriate stations, turn-back station locations must be constrained. That is

$$1 < a < m < b < n \quad \{a,m,b,n \in \text{N}^+\} \quad (41)$$

(6) Variable integer constraint

$$f_1, f_2, f_3, a, b, c, m, n \in Z^+ \quad \forall f_i \in [f_{\min}, f_{\max}] \quad (42)$$

IV. Solution Algorithm

TO train scheduling model constitutes a large-scale integer programming problem where computational complexity increases exponentially with station quantity X_i on the line. Based on the constructed TO scheduling model, we designed a chaotic non-dominated sorting genetic algorithm (CNSGA) incorporating oppositional learning for optimization. Compared with conventional genetic algorithms, CNSGA employs chaotic mapping instead of random number generators (applied in population initialization, crossover operators, and mutation operators), effectively avoiding local optima pitfalls.

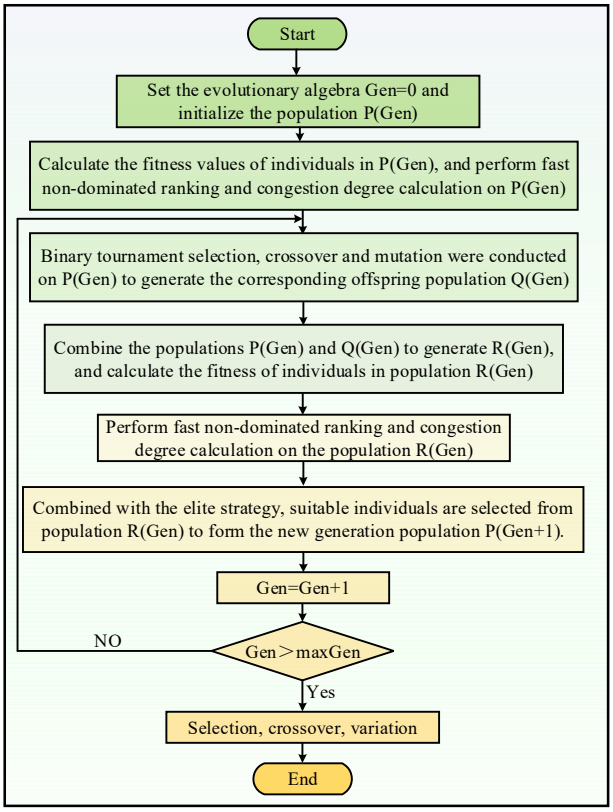

Fig.5. Algorithm flowchart of CNSGA.

A. Strategy for Generating Initial Solutions from Chaotic Maps Based on Oppositional Learning

Genetic algorithm performance is primarily evaluated through global convergence and convergence speed. The initial solution strategy using oppositional learning-based logistic L_{21}, L_{22} chaotic mapping helps overcome premature convergence and enhances population diversity. The logistic mapping iteration equation is

$$X_{i+1} = r \cdot X_i \cdot (1 - X_i) \quad (43)$$

Where, X_i represents the mapping value at the i-th generation; $x_i + 1$ denotes the updated mapping value at the $i+1$-th generation; r is the control parameter with value 4.

By introducing generalized opposition-based learning strategy, the algorithm simultaneously searches current positions and oppositional positions during population initialization. Let OP_i represent the oppositional particle of particle X_i:

$$OP_i = K \cdot (X_{\min}^D + X_{\max}^D) - X_i \quad (44)$$

Where, K denotes a random number, $K \in (0,1)$; $X_{\min}^D, X_{\max}^D$ indicate lower and upper bounds in the D-dimensional search space.

To ensure positivity of oppositional particle relative values, constraints are applied:

$$OP_i = -OP_i \cdot oper(0.5 + rand/2), \text{OP}_i < 0 \quad (45)$$

Where, $rand$ represents a random number, $rand \in (0,1)$; Simulation analysis from [21] demonstrates optimal algorithm convergence when $operation(\bullet)$ takes value [0.5,1].

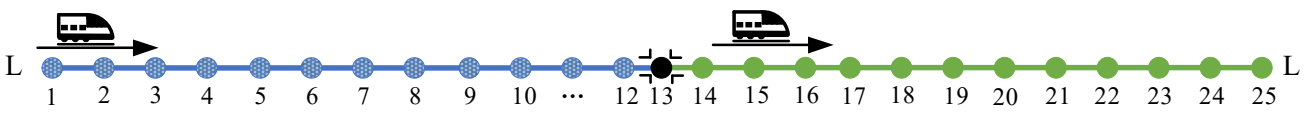

Fig.6. Circuit diagram.

B. Cross and mutation based on logistic chaotic mapping

If random number *rc* is smaller than crossover probability pc, the algorithm executes simulated binary crossover (SBX) operations following

$$x_{c1}^{i}=\frac{1}{2}[(1-\beta)x_{p1}^{i}+(1+\beta)x_{p2}^{i}] \tag{46}$$

$$x_{c2}^{i}=\frac{1}{2}[(1+\beta)x_{p1}^{i}+(1-\beta)x_{p2}^{i}] \tag{47}$$

$$\beta=\begin{cases}(2u)^{1/(\eta_c+1)}, & if\ u\le 0.5\\ (1/2(1-u))^{1/(\eta_c+1)}, & other\end{cases} \tag{48}$$

Where, u is a random number between 0 and 1, which is an indicator of the crossover operator and is generated using logistic chaotic mapping $u=X_i^j$.

If the generated random number rm is smaller than mutation probability pm, mutation operation is performed. For solution X_s, the mutation follows

$$X_s^*=X_s+(X_s^u-X_s^l)\times\delta_s \tag{49}$$

$$\delta_s=\begin{cases}(2u_s)^{1/(\eta_m+1)}, & if\ u_s\le 0.5\\ (1/2(1-u_s))^{1/(\eta_m+1)}, & other\end{cases} \tag{50}$$

Where, u_s is a random number between 0~1, A denotes the crossover operator index generated by logistic chaotic mapping, that is $u_s=X_i^j$.

The CNSGA flowchart is shown in Fig 5.

V. Case Studies

The L_S line of a certain city's rail transit has 13 stations $r=\{13,..,28\}$. The L_R line of the suburban railway has 16 stations $s=\{1,2...,13\}$. The station collections are respectively, and the URT line and the suburban railway pass through the junction station 13 to achieve seamless operation. The parameters of the weight function under profit conditions: δ=0.72, ρ=1.19; otherwise δ=0.76, ρ=1.21. The composition of different types of trains: $B_{s1}=B_{s2}=B_r$ =7. The fixed capacity of trains is 1460 people, the full load rate $\beta_r=\beta_s$=0.8, the turnaround time of trains at turnaround stations t_{turn}=4 min, the minimum turnaround time interval t_{zh}=2 min, and the passenger transfer travel time T_h=0.5 min. Distances: L_S=32 km, L_R=28 km. The minimum departure frequency $f_{r\min}$ A= $f_{s\min}$=5 pair/h, designed throughput capacity $N_r^{cap}=N_s^{cap}$=30 pair/h, fixed vehicle cost per unit time C_r=45 yuan/vehicle-hour, C_s=40 yuan/vehicle-hour, system operating cost per vehicle-kilometer e_r=12 yuan/vehicle-kilometer, e_s=10 yuan/vehicle-kilometer. The schematic diagram of the circuit is shown in Fig. 6. The study period was selected as the peak hour. Passenger flow data is shown in Fig. 7.

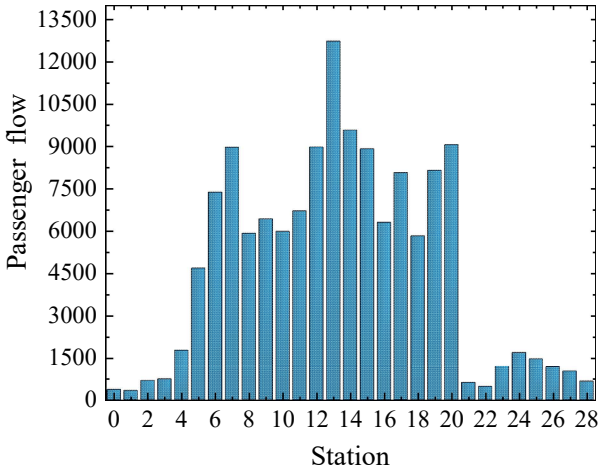

(a) Full day section passenger flow

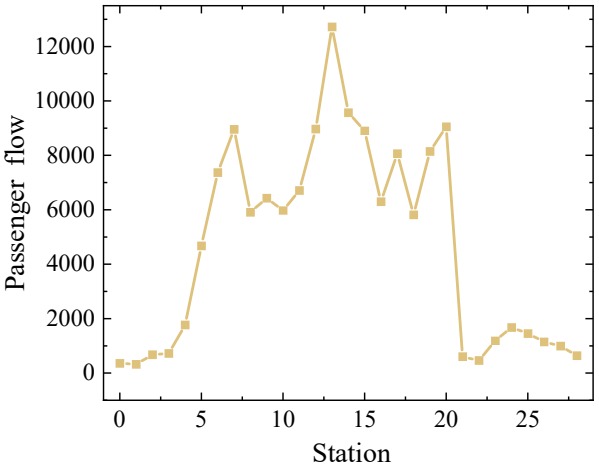

(b) Full day morning peak section passenger flow

Fig.7. Analysis of long-term Peak-hour Passenger flow data.

As shown in Fig. 7, the distribution of inbound passenger flow throughout the day follows a unimodal pattern with significant morning peak characteristics. The morning peak period of the line L_S is approximately 06:30-09:00, and the morning peak period of the line L_R is approximately 07:00-09:00. The selected study period is 07:00-08:00.

A. Model solution results

We used the Python 3.9.13 programming platform to solve the model using the MOPSOCO algorithm. The parameters were: population size M=200, external storage quantity N =100, acceleration constant C_2=0.3, and inertia weight coefficient $\varpi_{\min}$=0.4. The iteration process of the objective function value is shown in Fig. 8.

As shown in Fig. 8, the designed CNSGA algorithm effectively solves the target problem. As passenger total travel time increases, enterprise total cost gradually decreases, indicating a trade-off relationship between the two objectives due to target conflicts.

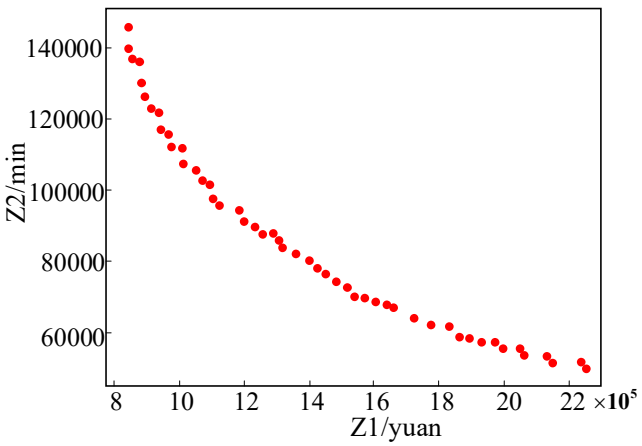

(a) Pareto front set

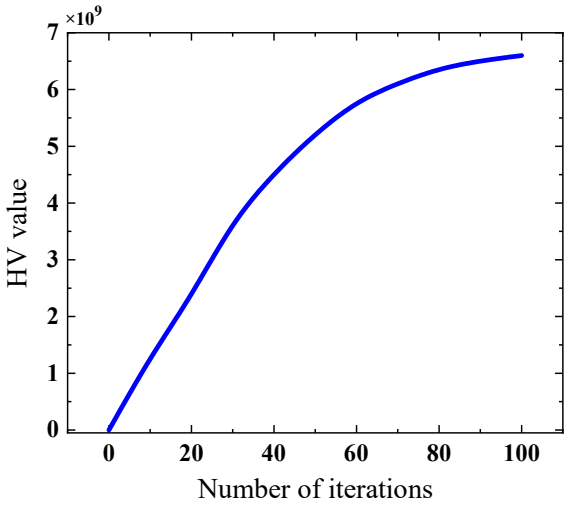

(b) HV iteration curve graph

Fig.8. The double objective iterative curve is set with pareto frontier.

B. Comparison of Different Schemes

The optimal solution for enterprise cost (Solution A), intermediate solution (Solution B), and optimal solution for passenger time (Solution C) were selected to analyze the Pareto frontier. The operation schemes corresponding to these solutions are shown in Fig. 9.

Fig. 9(a) shows that Solution A (enterprise cost optimum) minimizes transport costs by reducing train frequencies and through-route length. However, this compromises passenger comfort, service level, and time savings. This scheme is suitable only for transitional stages with limited resources.

Fig. 9(b) shows that Solution B (intermediate) is a balanced solution. Maintaining service levels with through-section [7,20], it maximizes passenger flow coverage while balancing passenger time and enterprise cost.

Fig. 9(c) shows that Solution C (passenger time optimum) maximizes through-route coverage and increases train frequencies to reduce travel time and improve service quality. However, this requires more vehicles, increases purchase costs, causes urban section congestion, and significantly raises operating costs.

After analyzing these solutions, we constrained train load factors to <100% and adopted fuzzy logic to select the ideal solution from the Pareto front (Fig. 10). Fig. 10 shows that the ideal solution falls within the compromise range, selecting the same through-section as Solution B but with optimized frequencies. This reduces enterprise costs while improving passenger service levels, and is adopted as the optimal solution.

The dual-objective values converged around 200 generations, with the total passenger travel time cost being 64,699.9 minutes and the total enterprise operating cost reaching 230,907.67 yuan. The stopping scheme for trains running through regional [5,20] is [1,0,1,1,0,1,1,1,0,1,0,1,1]. When passenger flow and other parameters remain unchanged, under the traditional transfer operation mode, the peak-hour operation frequency for Line [missing identifier] is [missing value] trains, and the operation frequency for Line [missing identifier] is [missing value] trains. A comparison of the operation plans before and after optimization is shown in Table 1.

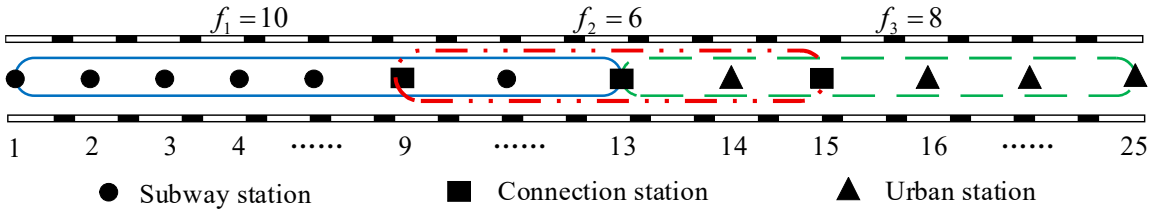

(a) Scheme A- Optimal Solution for the total cost of the enterprise

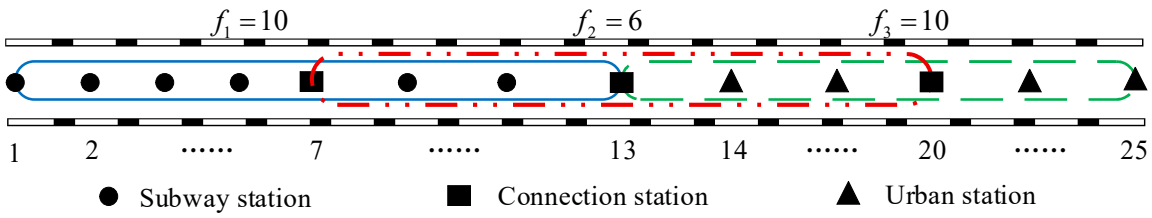

(b) Scheme B- Intermediate solution

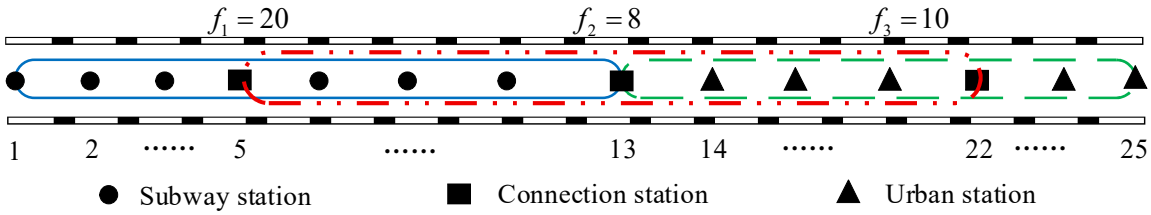

(c) Scheme C - Optimal Solution for Total Passenger time

Fig 9 Three special solutions

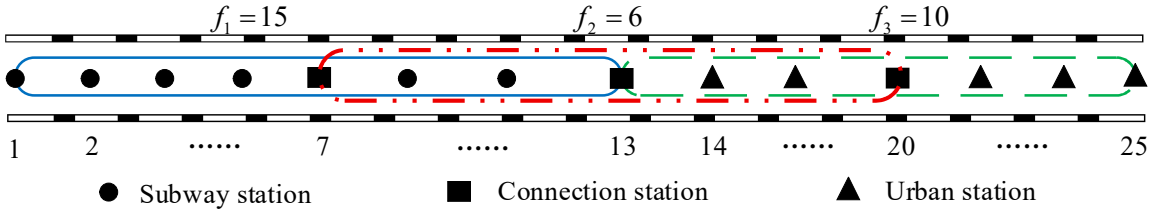

Fig 10 Ideal Solution

TABLE I
THE COMPARISON OF THE OPERATING PLAN RESULTS BEFORE AND AFTER OPTIMIZATION

operation scheme	Z1/min	Relative savings	Z2/yuan	Relative savings
Integrated operation	64699.98	60.7%	230907.67	30.1%
Transfer connection	164691.76	--	330498.06	--

According to Tab.1, compared to the traditional transfer and connection mode, the TO train operation plan saves 60.7% and 30.14% in Z1 and Z2, respectively. According to the data analysis results, the operation of through trains has brought savings to both passengers and enterprises, verifying the feasibility of the constructed operation plan. According to Table 1, compared to the TO station stop mode, the TO cross station stop mode saves 19.26% in passenger travel costs, but increases 1.89% in enterprise operating costs. Therefore, the integrated operation and cross station stop mode have a dual impact on passengers and businesses. Compared with the transfer connection mode, it can significantly reduce the travel time of CL passengers. However, compared with the TO station stop mode, due to the complex operational organization conditions required, the operating costs of enterprises actually increase.

VI. PARAMETER ANALYSIS

A. Cross station stop mode saves travel time for different passenger flows

To analyze skip-stop mode's impact on travel time across passenger flow types, the proportions of HMM, HKM, HMK, HKK, CMM, CMK, CKM, and CKK flows relative to total passenger volume were calculated. Simultaneously, the average travel times of these eight flow types under skip-stop and all-stop modes were compared. Travel time savings comparisons under different modes are shown in Fig. 10.

As seen in Fig. 11, the skip-stop mode demonstrates significant advantages in improving travel efficiency. Further analysis shows that CKK and HKK passenger flows achieve substantial time savings of 2.36/min and 5.13/min respectively through skip-stop operations. However, for CKM, CMK, and SKM passenger flows, time savings are relatively small, and travel time may even increase (HMK, HMM, CMM).

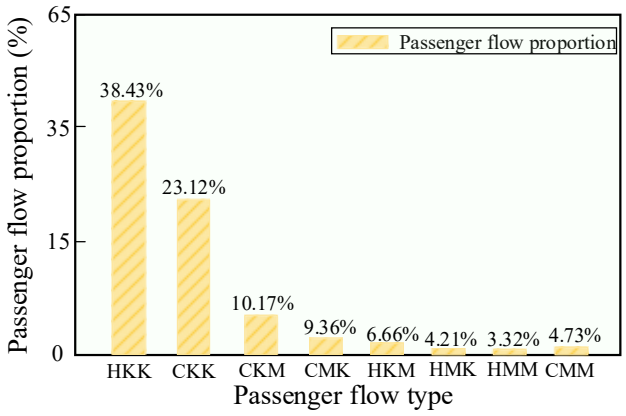

(a) Proportion of passenger flow types

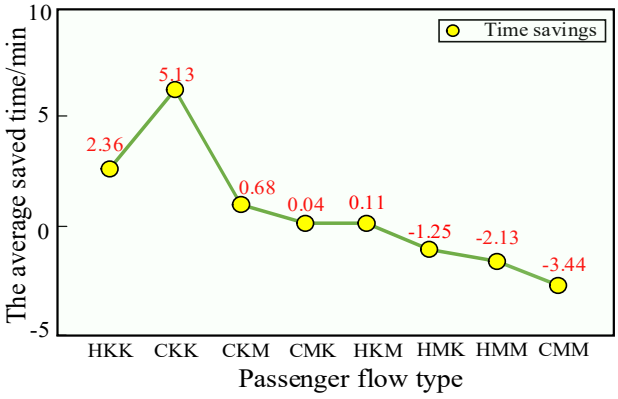

(b) Average time saved by various types of passenger flow

Fig.11. Comparison of travel time savings in different modes.

B. The impact of profit sensitivity coefficient α, loss sensitivity coefficient β, discrimination parameter σ, and attractiveness parameter ρ on the cumulative prospect value

Considering the impact of relevant key parameters in the value function on the cumulative prospect value, the influence of these key parameters is shown in Fig. 12.

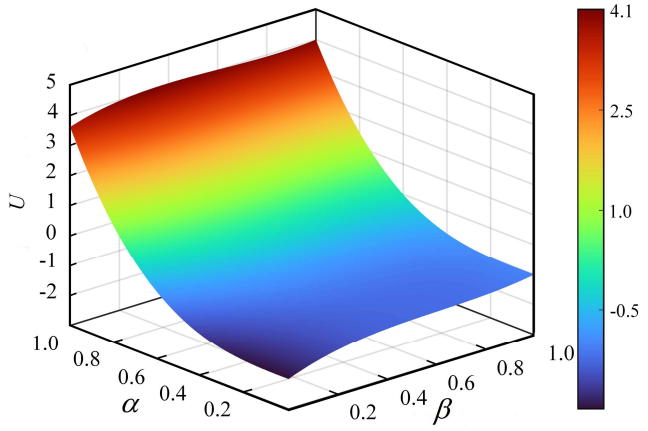

(a) Effect of Parameters α、β on U

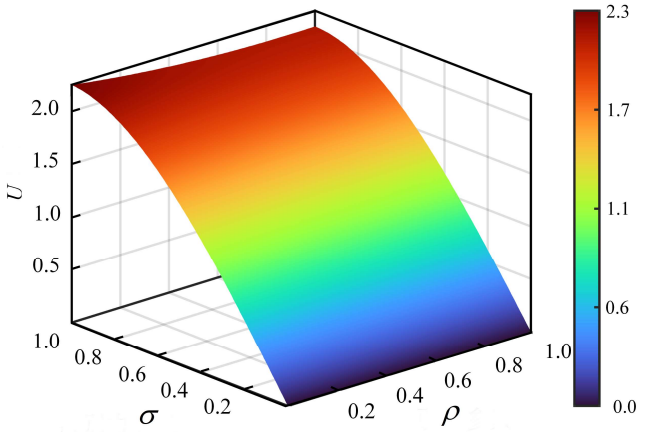

(b) Effect of Parameters σ、ρ on U

Fig. 12. The Influence of Key Parameters in the Value Function on the Cumulative Prospect Value U.

As shown in Fig. 12, the cumulative prospect value U increases with the increase of α and β. Meanwhile, it can be seen that the gain sensitivity coefficient α has a greater impact on the cumulative prospect value than the loss sensitivity coefficient β. This indicates that when path travel time is less than passengers' expectations, passengers tend to exhibit risk-averse psychology. Simultaneously, the cumulative prospect value U increases with the increase of σ but decreases with the increase of ρ. This demonstrates that the discriminability parameter σ has a far greater influence on the cumulative prospect value than the attractiveness parameter ρ.

C. The impact of time value on passenger selection probability

To explore the complex mechanism of mutual influence between passengers' time value and choice probability, we take the time value *vot* (*k*) of passengers choosing through trains as an example, analyze the changes under different *vot* (*k*) values. The impact of time value on passenger choice probability is shown in Fig. 13(a) and 13(b).

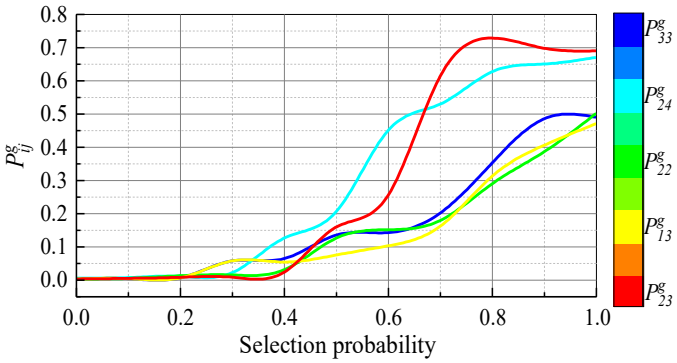

(a) Profile P_{ij}^g of the Influence of vot (g) Pair

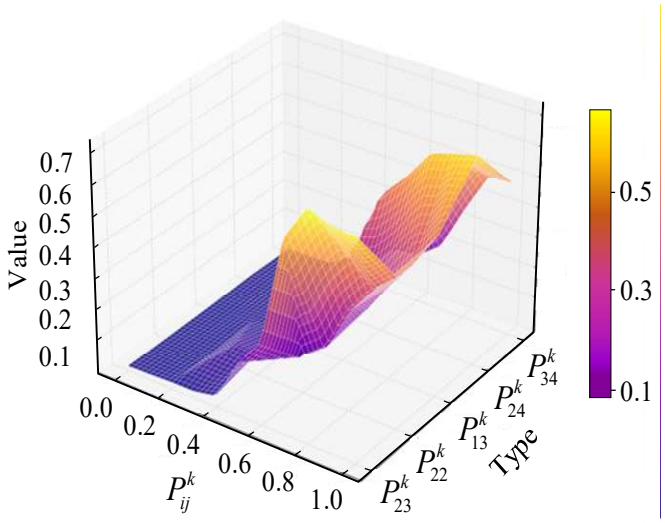

(b) Three dimensional Line Chart of the Influence of *vot* (*g*) Pair

Fig.13. The influence of the value of time on the probability of passengers choice.

As shown in Fig. 13, the probability of passengers choosing through trains is positively correlated with the time value *vot* (*k*). When *vot* (*k*) > 0.5, the probability of passenger flows between [D2, D3] and between [D2, D4] choosing through trains is the highest, indicating their most urgent demand for through trains. Therefore, when *vot* (*k*) > 0.5 and there exists significant CL passenger flow, operating through trains has higher necessity; whereas when *vot* (*k*) ≤ 0.5, the probability of passengers choosing through trains is relatively low, and the demand for operating through trains is relatively small. In summary, when passengers' time value is high, operating through trains can effectively meet travel demands and improve transportation efficiency. In actual rail transit operations, through-train operation plans should be reasonably formulated based on passengers' time value and flow characteristics to maximize operational benefits.

D. The disurbance effect of the ratio of vot (g): vot (b) on the operation plan

The proportion of time value *vot*(*g*) for passengers choosing through trains to time value *vot*(*b*) for passengers choosing local trains can be divided into three cases: 0<*vot*(*g*):*vot*(*b*)<1, *vot*(*g*):*vot*(*b*)=1, and *vot*(*g*):*vot*(*b*)>1.We take Pareto solutions under different ratios of *vot*(*g*):*vot*(*b*) to compare the impact on operation plans before and after considering passenger travel time value. The Pareto solution sets under different *vot*(*g*):*vot*(*b*) values are shown in Fig. 14.

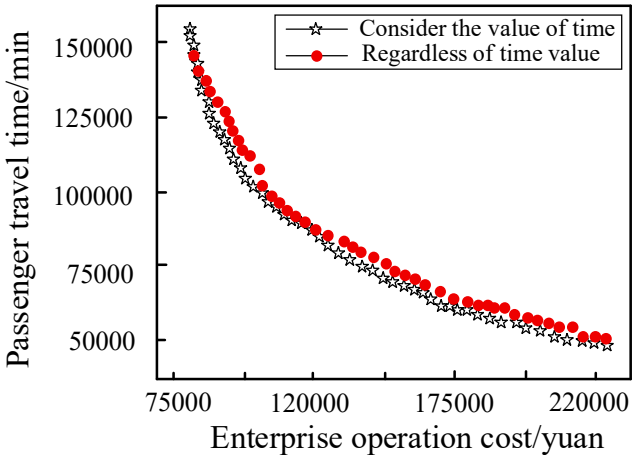

(a) Pareto solution at *vot* (*g*): *vot* (*b*)=0

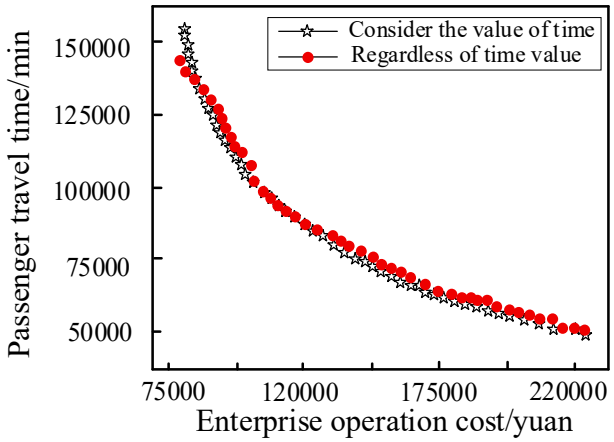

(b) Pareto solution at *vot* (*g*): *vot* (*b*)=1

According to Fig. 14, it can be seen that when the time value ratio is 0.5 (Fig. 14a), the curves before and after considering the time value basically overlap, indicating that the difference in passenger time value has a weak impact on the optimization results at this time. As the ratio increases to 1 (Fig. 14b), the two curves begin to separate, and the solution considering time value shows a downward trend in both operating costs and passenger travel time.

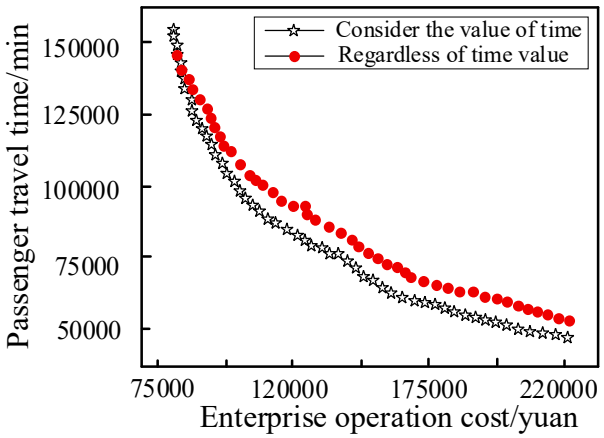

(c) Pareto solution at *vot* (*g*): *vot* (*b*)=1.5

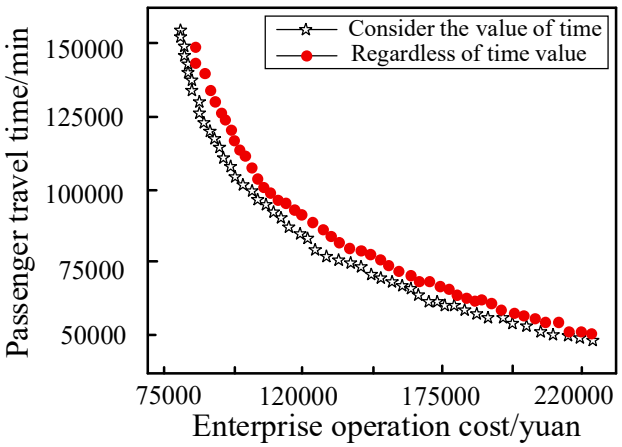

(d) Pareto solution at *vot* (*g*): *vot* (*b*)=2

Fig.14. The impact on the operation plan before and after considering the value of time.

When the ratio further increases to 1.5 (Fig. 14c) and 2 (Fig. 14d), the curve spacing significantly widens, and the red curve (considering time value) shifts significantly to the left on the passenger travel time cost axis compared to the black curve (not considering time value), indicating that the increase in time value difference would enhance the optimization effect: a higher *vot* (*g*): *vot* (*b*) ratio prompts the TO plan to be more inclined to reduce the travel time cost of high time value passengers, while adjusting the operation plan to achieve an effective balance of total system cost, verifying the leverage effect of time value difference in collaborative optimization operation efficiency and passenger travel.

E. The influence of operating frequency on different types of passenger flows

The operating frequencies of three train types differentially impact passenger flows. To analyze this, adjustment plans for departure frequencies are denoted as $F(\Delta f_1, \Delta f_2, \Delta f_3)$. Changes in average travel time per OD interval and passenger flow attraction under frequency adjustments were examined. Impacts on different passenger types are shown in Fig. 15.

As seen in Fig. 15, passengers traveling within $[D_1 - D_3]$ and $[D_2 - D_3]$ intervals are most sensitive to through-train frequency f_2. When f_2 increases (e.g., Scheme F(-1,2,-2)), the proportion of CL passenger flow (passengers in $[D_1 - D_3]$ and $[D_2 - D_3]$) increases by 12%. $[D_1 - D_1]$ passengers are more sensitive to f_1, while $[D_4 - D_4]$ passengers are mainly affected by f_3. However, overall, passenger flows within urban rail and regional lines remain relatively "quiet": average travel time fluctuates only ±2min, with flow proportion stabilizing at 20%-25%, indicating service saturation. Therefore, increasing f_2 attracts more passengers to choose through trains while reducing CL travel time.

However, extreme frequency adjustments cause flow imbalance. Scheme *F*(-1,2,-2) increases travel time for

$[D_4 - D_4]$ passengers by 28% and decreases flow proportion by 8%. When reducing f_3 in Scheme $F(3,0,-1)$, $[D_3 - D_4]$ travel time increases by 22%, with flow shifting to $[D_2 - D_3]$. Thus, excessive increase of f_2 with reduction of f_1 / f_3 may cause insufficient service in certain sections, prolonged travel times, or flow imbalance.

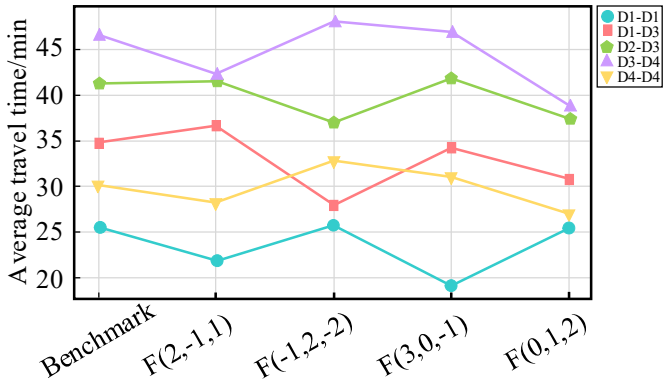

(a) Impact on average travel time

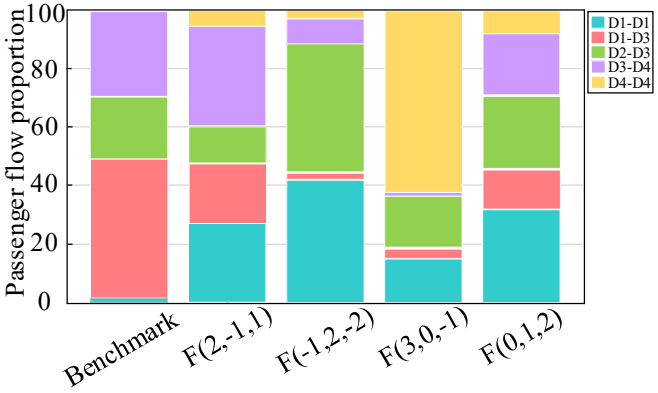

(b) The degree of attraction to passenger flow

Fig 15. The impact of the operation frequency adjustment scheme on different types of passenger flows

F. Fairness Analysis of Through Operation

Through trains consume partial resources of local lines. To analyze the impact of through-train operation on urban rail local lines and suburban railway local lines, and to explore the fairness of through operation, variations in travel time change rates for passengers across different zones are illustrated in Fig 16.

s shown in Fig 16(a), passenger travel time changes exhibit a distinct spatial gradient: the most significant increase occurs in the urban rail line segments (Stations 1-5), forming a red high-impact zone. The impact gradually diminishes as stations extend towards the suburbs (Stations 5-13). The cross-line zones (Stations 14-20) form a blue valley with significantly reduced times, while the impact levels off in the outer suburban areas (Stations 22-28). This demonstrates that passengers in the urban core bear the primary negative effects, whereas those in cross-line zones gain the most benefits, reflecting the efficiency-fairness trade-off in transportation system optimization.

As seen in Fig 16(b), a striking "twin-peak and single-valley" topography emerges: the urban core (Stations 4-8) appears as a red peak, while the cross-line zone (Stations 14-20) forms a blue valley, visually illustrating the differential impacts of through operation. The magnitude of time change increases with proximity to the city center and attenuates with distance, indicating greater sensitivity to operational adjustments among central urban passengers.

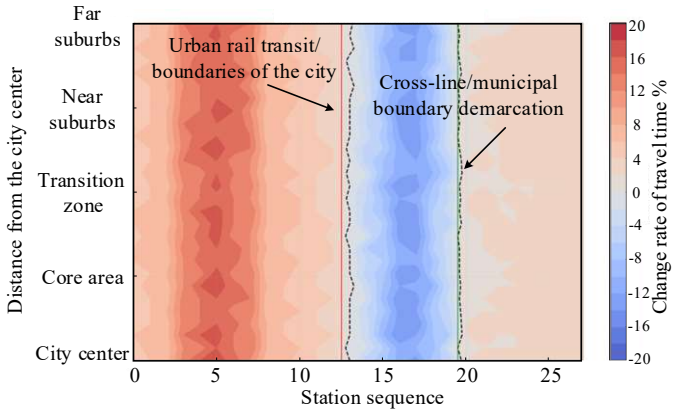

(a) Contour maps of the rate of change in passenger travel time in different regions

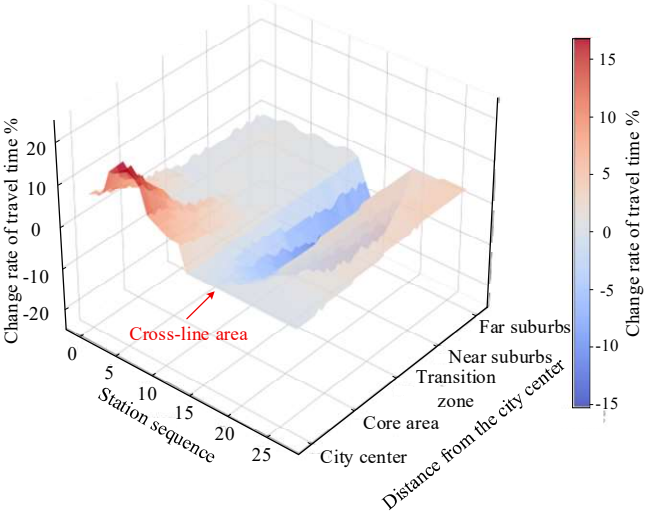

(b) A three-dimensional surface graph of the change rate of passengers' travel time in different regions

Fig 15. The variation in the rate of change of passengers' travel time in different regions

Therefore, while through operation resolves efficiency losses in cross-modal connections through spatiotemporal resource redistribution, it partially transfers costs to local-line passengers. This inherent "efficiency gains-cost shifts" trade-off in multi-level rail network coordination requires improvement through scheduling and demand management.

VII. Conclusion

1) This study innovatively applies CPT-QDT theory to URT-SR through-operation research, constructing an optimization model integrating multi-attribute passenger behavior. It reveals complex mechanisms of passenger flow allocation and operational resource coordination under bounded rationality, providing theoretical basis for multi-level rail network coordination. Practical applications require dynamic parameter adjustments based on line characteristics to enhance model adaptability.

2) Compared to transfer mode, through-operation reduces average CL travel time by 8.32min, with total passenger travel time and enterprise operating costs reduced by 60.7% and 30.1% respectively.

3) Parameter analysis indicates, Passengers with high time value show greater preference for through trains, and an increased time value ratio significantly enhances optimization effects. While skip-stop patterns reduce overall passenger travel time, their potential negative impacts on certain passenger flows require careful trade-offs. Although through operation improves cross-line efficiency, it transfers time costs to urban core passengers, creating a spatial disparity characterized by "efficiency gains-cost shifts." Future efforts should focus on targeted optimization of scheduling strategies to enhance equity across regions.

4) Future research should: integrate real-time passenger data; develop time-varying parameter frameworks to enhance adaptability to sudden demands; explore coordination mechanisms between through-operation and other transport modes; thereby improving regional transport network resilience.

REFERENCES

[1] C. Zhu, X. Yang, Z. Wang, J. Fang, J. Wang, L. Cheng, "Optimization for the train plan with flexible train composition considering carbon Emission," *Engineering Letters*, vol. 31, no. 2, pp. 562-573, 2023.

[2] H. Wu, J. Zhen, J. Zhang, "Urban rail transit operation safety evaluation based on an improved CRITIC method and cloud model," *Journal of Rail Transport Planning & Management*, vol. 16, Article ID 100206, 2020.

[3] Ito. M, "Through service between railway operators in Greater Tokyo," *Japan Railway & Transport Review*, vol. 63, pp. 14-21, 2014.

[4] Vigrass. J. W, "Alternative forms of motive power for suburban rail rapid transit," *In ASME/IEEE Joint Conference on Railroads*, pp. 65-77, 1990.

[5] Drechsler. G, "Light railway on conventional railway tracks in Karlsruhe, Germany," *In Proceedings of the Institution of Civil Engineers-Transport*, Vol. 117, no. 2, pp. 81-87, 1996.

[6] Sato. L, Essig. P, "How Tokyo's Subways Inspired the Paris RER," *Japan Railway & Transport Review*, vol. 23, PP. 36-42, 2000.

[7] Novales. M, Orro. A, Bugarin. M, "Madrid tram-train feasibility study conclusions," *Proceedings of the Institution of Mechanical Engineers, Part F: Journal of Rail and Rapid Transit*, Vol. 217, no. 1, pp. 1-10, 2003.

[8] L. Tang, X. Xu, "Optimization for operation scheme of express and local trains in suburban rail transit lines based on station classification and bi-level programming," *Journal of Rail Transport Planning & Management,* Vol. 21, Article ID 100283, 2022.

[9] L. Tang, A. D'Ariano, X. Xu, et al. "Scheduling local and express trains in suburban rail transit lines: Mixed–integer nonlinear programming and adaptive genetic algorithm," *Computers & Operations Research*, Vol. 135, Article ID 105436, 2021.

[10] Parbo. J, Nielsen. O. A, Prato. C, "Reducing passengers' travel time by optimizing stopping patterns in a large-scale network: A case-study in the Copenhagen Region," *Transportation Research Part A: Policy and Practice*, Vol. 113, pp. 197-212, 2018.

[11] Altazin. E, Dauzère-Pérès. S, Ramond. F, et al. "Rescheduling through stop-skipping in dense railway systems," *Transportation Research Part C: Emerging Technologies*, Vol. 79, pp.73-84, 2017.

[12] P. Shang, R. Li, Z. Liu, et al. "Timetable synchronization and optimization considering time-dependent passenger demand in an urban subway network," *Transportation Research Record*, Vol. 2672, no. 8, pp. 243-254, 2018.

[13] A. Yang, B. Wang, J. Huang, "Service replanning in urban rail transit networks: Cross-line express trains for reducing the number of passenger transfers and travel time," *Transportation Research Part C: Emerging Technologies*, Vol. 115, Article ID 102629, 2020.

[14] Yang. A, Huang. J, Wang. B, et al. "Train scheduling for minimizing the total travel time with a skip-stop operation in urban rail transit," *IEEE Access*, Vol. 7, pp. 81956-81968, 2019.

[15] Tang. L, Xu. X, "Optimization for operation scheme of express and local trains in suburban rail transit lines based on station classification and bi-level programming," *Journal of Rail Transport Planning & Management*, Vol. 21, Article ID 100283, 2022.

[16] Li. Z, Mao. B, Bai. Y, et al. "Integrated optimization of train stop planning and scheduling on metro lines with express/local mode," *IEEE Access*, Vol. 7, pp.88534-88546, 2019.

[17] Chen. Z, Li. S, D'Ariano. A, et al. "Real-time optimization for train regulation and stop-skipping adjustment strategy of urban rail transit lines," *Omega*, Vol. 110, Article ID 102631, 2022.

[18] Shao. J, Xu. Y, Sun. L, e tal. "Equity-oriented integrated optimization of train timetable and stop plans for suburban railways system," *Computers & Industrial Engineering*, Vol. 173, Article ID 108721, 2022.

[19] Zhu. T, Su. Y, Huang. T, "A dimension reduction classification method combining chaotic mapping and genetic algorithm for Zhuhai-1 hyperspectral images," *In International Conference on Wireless Communications, Networking and Applications*, pp. 384-389, 2022.

[20] Lu. H, Niu. R, Liu. J, Zhu. Z, "A chaotic non-dominated sorting genetic algorithm for the multi-objective automatic test task scheduling problem," *Applied Soft Computing,* vol. 13, no. 5, pp.2790-2802, 2013.

[21] Jiao. C, Yu. K, Zhou. Q, "An opposition-based learning adaptive chaotic particle swarm optimization algorithm," *Journal of Bionic Engineering*, vol.21, pp. 3076–3097, 2024.

[22] Zhan. Y, Ye. M, Zhang. R, He. S, & Ni. S, "Multi-objective optimization for through train service integrating train operation plan and type selection," *Transportation Letters*, vol. 16, no. 9, pp. 1039-1058, 2024. https://doi.org/10.1080/19427867.2024.2268754.

[23] Kang. L, Lai. Y, Wang. J, Cao. W, "A Pacesetter-Lévy multi-objective particle swarm optimization with Arnold Chaotic Map with opposition-based learning," *Information Sciences,* vol. 678, pp. 121048, 2024.

[24] Di. X, Liu. H. X, "Boundedly rational route choice behavior: A review of models and methodologies". *Transportation Research Part B: Methodological*, vol. 85, pp. 142-179, 2016.

[25] Kahneman. D, Tversky. A, "Prospect theory: An analysis of decision under risk," *In Handbook of the Fundamentals of Financial Decision Making: Part I*, pp. 99-127, 2013.

[26] Gao. S, Frejinger. E, Ben-Akiva. M, "Adaptive route choices in risky traffic networks: A prospect theory approach," *Transportation Research Part C: Emerging Technologies*, vol. 18, no. 5, pp. 727-740, 2010.

[27] Xu. H, Lou. Y, Yin. Y, & Zhou. J, "A prospect-based user equilibrium model with endogenous reference points and its application in congestion pricing," *Transportation Research Part B: Methodological*, vol. 45, no. 2, pp. 311-328, 2011.

[28] Zhang. C, Liu. T. L, Huang. H. J, & Chen. J, "A cumulative prospect theory approach to commuters' day-to-day route-choice modeling with friends' travel information," *Transportation Research Part C: Emerging Technologies*, vol. 86, pp. 527-548, 2018.

[29] Hensher. D. Areene. W. H, Li. Z, "Embedding risk attitude and decision weights in non-linear logit to accommodate time variability in the value of expected travel time savings," *Transportation Research Part B: Methodological*, vol. 45, no. 7, pp. 954-972, 2011.

[30] Ghader. S, Darzi. A, Zhang. L, "Modeling effects of travel time reliability on mode choice using cumulative prospect theory," *Transportation Research Part C: Emerging Technologies*, vol. 108, pp. 245-254, 2019.

[31] Avineri. E, "A cumulative prospect theory approach to passengers behavior modeling: waiting time paradox revisited," *In Intelligent Transportation Systems*, Vol. 8, no. 4, pp. 195-204, 2004.

[32] Martínez-Martínez. I, "A connection between quantum decision theory and quantum games: The Hamiltonian of strategic interaction," *Journal of Mathematical Psychology*, vol. 58, pp. 33-44, 2014.

[33] Moreira. C, Wichert. A, "Quantum probabilistic models revisited: The case of disjunction effects in cognition," *Frontiers in Physics*, vol. 4, no. 26, 2016.

[34] Pothos. E. M, Busemeyer. J. R, "A quantum probability explanation for violations of 'rational' decision theory," *Proceedings of the Royal Society B: Biological Sciences*, vol. 276, no. 1665, pp. 2171-2178, 2009.

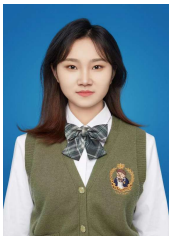

Shuoyue Gao was born in Shaanxi, China. She received her Bachelor's degree in Traffic and Transportation from Shijiazhuang Tiedao University, China, in 2023. Currently, she is pursuing a Master's degree in Traffic and Transportation (Railway Transportation Engineering) at Lanzhou Jiaotong University. Her research interests include through operations and passenger flow distribution.